International Journal of Multiphysics
Volume 18, No. 4, 2024
ISSN: 1750-9548

Fabrication of a Novel Electrochemical Sensor Using L-Cysteine-Glutaraldehyde-Glutamine-Cu^{2+} Self-Assembled Monolayer on a Gold Electrode for the Determination of Curcumin in Human Blood Serum

Mohammad Reza Baezzat[1]*, Abdul Reza Rahpeyma[1], Hossein Tavallali[1]

[1]Faculty of Chemistry, Payame Noor University, 19395-4697 Tehran, Iran

*Corresponding author: Mohammad Reza Baezzat

Abstract

In this study, a new electrochemical sensor based on self-assembled monolayers of Cys-GA-Gln-Cu^{2+} modified gold electrode was fabricated. The electrocatalytic activity of adsorbed copper ions was utilized to determine the quantitative concentration of curcumin. Techniques such as cyclic voltammetry (CV) and electrochemical impedance spectroscopy (EIS) with an external redox probe were used to investigate the layer-by-layer modification on the gold electrode surface. This electrode showed selective and reproducible adsorption for Cu^{2+}In the absence of curcumin, the DPV redox peak for Cu^{2+} was observed at about 276 mV with an anodic current of 1.36 µA vs. Ag/AgCl for 5.0×10^{-4} M of copper. In the presence of curcumin, an anodic peak was observed at 292 mV vs. Ag/AgCl with 3.86 µA for 5×10^{-4} M of Cu^{2+}. The results demonstrated that the electrocatalytic properties of copper in the presence of curcumin could be used as a precise sensor for the determination of trace concentrations of curcumin in human blood serum. The differential pulse voltammetric response of the modified SAM electrode was linear against curcumin concentration in the range of 1×10^{-6} to 1×10^{-10} M with an R^2=0.9982 at pH= 5. The relative standard deviation (RSD) determined by DPV was 4.1%. Advantages of the sensor include good sensitivity, selectivity, simple recovery, and an inexpensive preparation method. The detection limit could be estimated 1.31×10^{-11} M according to the IUPAC recommendation (3σ).

Keywords: Electrochemical sensor, Self-assembled monolayers, Curcumin, Electrochemical impedance spectroscopy, modified gold electrode sensor, Cyclic voltammetry

Introduction

Curcumin (CM) (1, 7-bis (4-hydroxy-3-methoxyphenyl)-1, 6-heptadiene-3, 5-Dione) (Fig. 1) is a polyphenolic compound derived from turmeric, the rhizome of the Curcuma longa plant [1]. This compound exhibits anti-inflammatory, anticoagulant [2], and antitumor properties [3, 4]. The main origin of the turmeric plant is eastern India and China. However, it is also cultivated in many tropical areas, such as Malaysia, Indonesia, Pakistan, Africa, and South America [5-7]. The yellow color of turmeric is mainly due to a group of polyphenols called curcuminoids. Curcumin, demethoxycurcumin, and bisdemethoxycurcumin are the curcuminoids in turmeric, which differ in terms of the substitution of the methoxy group on the aromatic rings in their structures [8-10]. Curcumin is the most active component of turmeric and is also its main therapeutic agent [11-12]. Various studies have demonstrated the therapeutic benefits of curcumin, including its anti-inflammatory [13], antibacterial [14], and antioxidant properties [15], and its ability to heal wounds and infections [16]. Additionally, curcumin has been used to treat diseases such as allergies, depression, colitis, diabetes, nephrotoxicity, Alzheimer's, psoriasis, cardiovascular diseases, multiple sclerosis (MS), and AIDS [17-20]. Active oxygen radicals, including superoxide

and hydroxyl radicals, contribute to the development of arteriosclerosis and carcinogenesis. Therefore, eliminating these active radicals is effective in preventing cardiovascular diseases and cancers [21-24]. Compared to vitamins C and E, curcumin has a significantly more powerful antioxidant activity, inhibiting the synthesis of free radicals and facilitating their deactivation and removal [25-27]. One of the most important properties of curcumin is its high potential in preventing cancer development and aiding in the treatment of these diseases while reducing the unwanted side effects of chemotherapy [28, 29]. Curcumin exerts its anticancer activity by inhibiting inflammatory pathways, halting cellular cycles, inducing apoptosis, and inhibiting angiogenesis and metastasis in cancerous cells [30]. This compound has proved to be effective in treating a wide variety of cancers, including blood, prostate, uterus, lung, liver, kidney, ovarian, and pancreatic cancers [31-33]. Considering the positive characteristics of curcumin and its role in preventing and treating different diseases, it is crucial to find an effective method for its identification and quantification. Various analytical methods have been used for the detection of curcumin, including high-performance liquid chromatography [34], capillary electrophoresis [35], ultraviolet-visible spectroscopy [36], spectrofluorimetry [37], resonance light scattering [38], and electrochemical methods [39, 40]. Among these methods, electrochemical sensors have gained popularity due to their fast response, low cost, simple operation, high sensitivity, and suitable selectivity [41, 42]. However, the weak response of curcumin with traditional electrochemical sensors has always been a challenge. Therefore, modified electrodes are preferred for electrochemical measurement of curcumin [43-45]. Identifying appropriate compounds with high stability and good catalytic activity for modifying electrodes remains a significant challenge [46]. Chemical modification of electrode surfaces is crucial in electrochemistry, offering a wide spectrum of promising applications. In particular, thin films and self-assembled monolayers (SAMs) have been used in electroanalytical chemistry for electrode modification to develop sensors [47, 48] and biosensors [49, 50]. Recent studies have shown that incorporating metals or metal-binding units with desired electrical, magnetic, optical, and catalytic properties or molecular recognition abilities into gold–thiol SAMs can be used for the development and fabrication of sensors [51]. The catalytic and electrocatalytic behavior of copper cations for the oxidation or reduction of organic and biological compounds has been reported by several investigators. For example, several papers have been devoted to the catalytic [52, 53] and electrocatalytic [54-57] activity of Cu (II) for the redox reaction of p-benzoquinone/hydroquinone (PBQ/H_2Q). Shervedani et al. [58] studied the electrocatalytic activity of Au-5-amino-2-mercaptobenzimidazole-M^{n+} (Au-5A2MBI-M^{n+}) SAM complexes (where M^{n+} is a metal cation such as Cu^{2+} or Ag^{+}) for the oxidation reaction of hydroquinone (H_2Q) at pH 6 in an aqueous medium and concluded that Au-5A2MBI-Ag^{+} is a more efficient electrocatalyst than Au-5A2MBI-Cu^{2+} for the redox reaction of H_2Q [59]. In this study, the electrocatalytic activity of Cu^{2+} towards the oxidation reaction of curcumin is described. The catalyst is formed by immobilizing Cu (II) ions on the top side of a Gold-L-Cys-GA-Gln self-assembled monolayer electrode. The preparation steps and electrocatalytic activity of AuE-L-Cys-GA-Gln-Cu^{2+} have been studied by cyclic voltammetry and electrochemical impedance spectroscopy. The results show that the electrocatalytic properties of copper in the presence of curcumin can be used as a precise sensor for determining trace concentrations of curcumin in human blood serum (Fig. 2).

Fig. 1 Structure of curcumin

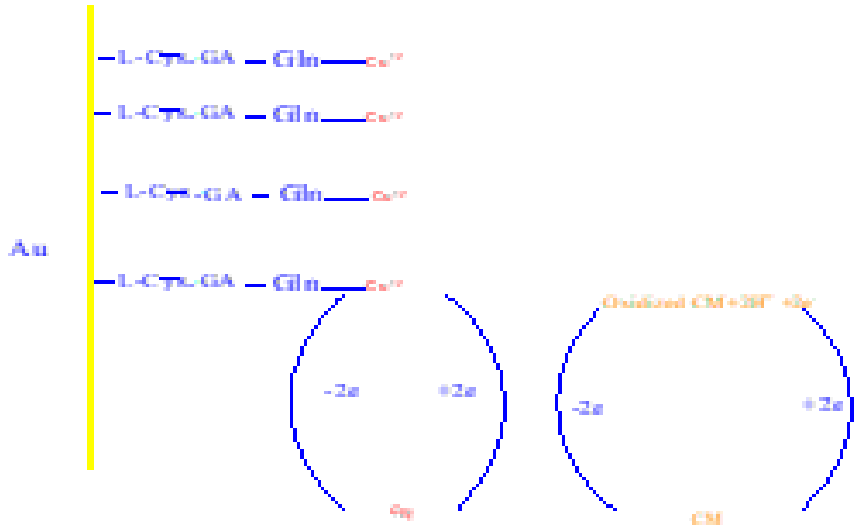

Fig. 2 Schematic diagram of the electrochemical involving Currcumin (CM), oxidized curcumin, cu and cu^{2+}reactions

2. Experimental

2.1. Materials and reagents

Analytical grade L-cysteine, Curcumin (CM) (pure powder), Glutaraldehyde ($C_5H_8O_2$, 25% v/v in water) (GA), Glutamine (Gln), EtOH, Cu $(NO_3)_2 \cdot 3H_2O$, H_2SO_4, KCl, Alumina powder for polishing, $K_4Fe(CN)_6 \cdot 3H_2O$ as a redox probe, and ETHylenediaminetetraacetic acid (EDTA) were obtained from Merck and used as received. Other chemicals were of analytical grade, obtained from commercial sources (Sigma-Aldrich or Merck), and used without further purification. All solutions were prepared with double-distilled water. Phosphate buffer solution (PBS) with the required pH was prepared by mixing 0.1 M KH_2PO_4/0.1 M K_2HPO_4, and the pH of the solution was adjusted with 0.1 M H_3PO_4 or 0.1 M NaOH. The test solutions were deaerated with high-purity nitrogen gas for 10 minutes before use and kept under a nitrogen atmosphere during the experiments. The gold electrode (99.99%, 0.0314 cm^2) was purchased from Azar Electrode Co. (Urmia, Iran).

2.2. Apparatus

The pH of the solutions was controlled with a Metrohm pH meter Model 713 using a glass electrode (Metrohm, Swiss). CV and impedimetric measurements were carried out using an Autolab electrochemical analyzer Model PGSTAT 302 N potentiostat/galvanostat (Eco-Chemie, Netherlands). The conventional three-electrode system comprised an Ag/AgCl (3.0 M KCl) reference electrode, a platinum counter electrode, and a gold working electrode. The electrochemical impedance spectra and voltammograms were analyzed using Nova 2.1.1 software. All electrochemical experiments were carried out in a three-electrode conventional system under room temperature (19 ◦C).

2.3. Preparation of modified electrode

The gold electrode (AuE) was carefully polished with an alumina slurry (0.3 and 0.05 mm) and then ultrasonically cleaned in double-distilled water (DDW) and ethanol. It was then electrochemically cleaned by cycling the electrode potential between 0.0 to +1.5 V vs. Ag/AgCl in 0.5 M H_2SO_4 until a reproducible voltammogram was obtained (Fig. 3) [60]. Finally, the electrodes were cleaned in freshly prepared “piranha” solution (a 1:3 (v/v) mixture of 30% H_2O_2 (30%) and concentrated H_2SO_4 (98%); Warning: Piranha solution is extremely corrosive and must be handled carefully) for 3 minutes and rinsed thoroughly with double-distilled water. The preparation of the AuE-L-Cys-GA-Gln electrode was performed in a three-step method: (i) immediately after cleaning, the bare

gold electrode (AuE) was immersed into an 18 mM L-Cys aqueous solution for 4 hours at room temperature in darkness to form AuE-L-Cys and washed with purified water to eliminate physically adsorbed L-cysteine; (ii) the AuE-L-Cys modified electrode was soaked in PBS (pH 6.0) containing 12% (v/v) GA solution for 1 hour to form AuE-L-Cys-GA and rinsed with water; (iii) the AuE-L-Cys-GA electrode was dipped into a 0.01 M Gln solution for 2 hours to form AuE-Cys-GA-Gln SAM by means of Schiff's base formation [61-65] between the aldehyde groups of GA and the amino groups of Gln. Lastly, the modified electrode (AuE-Cys-GA-Gln) was taken out, cleaned with water, and put to use in electrochemical tests(Fig. 4). In order to create Au-Cys-GA-Gln-Cu^{+2}, the Au-Cys-GA-Gln SAM-modified electrode was dipped into 10 ml of stirred solution containing the supporting electrolyte and the required concentration of Cu^{2+} with a defined pH. After that, the electrode was taken out, cleaned with PBS devoid of copper, and utilized right away for electrochemical experiments.

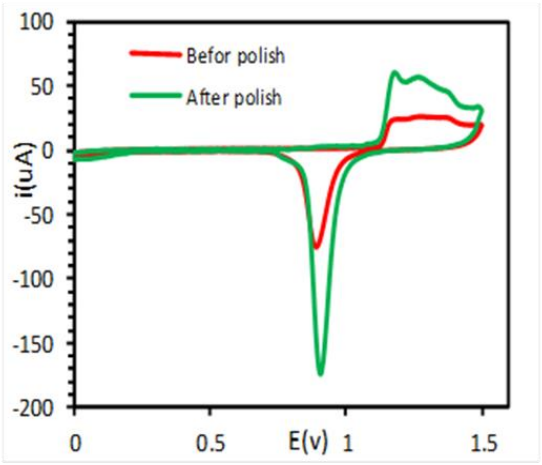

Fig. 3 Cyclic voltammograms obtained for electrochemical oxidation/reduction of Au in 0.5 M H_2SO_4

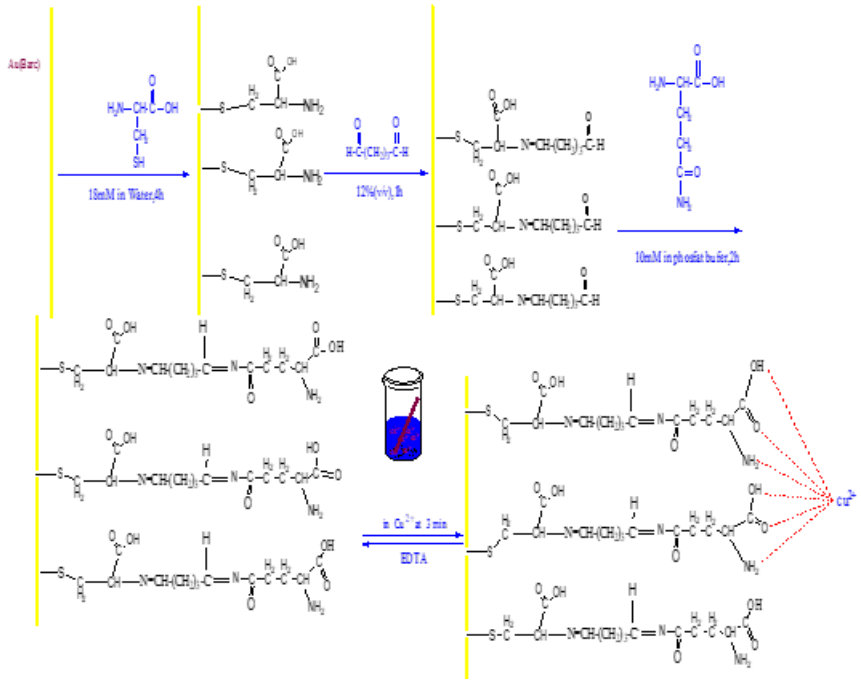

Fig. 4. Schematic representation of the proposed mechanism for the construction of the Au-Cys-GA-Gln-Cu^{2+} SAM electrode

2.4. Preparation of the human plasma samples

To evaluate the developed analysis method for application in real samples, the measurements were also performed in human plasma as a real sample provided by the Blood Transfusion Organization of Iran (Tehran). 1 mL of the provided sample was mixed with buffer at an optimum pH in a 10 mL volumetric flask. The standard addition method was utilized to determine CM. Before dilution, certain amounts of the standard solution were added to the sample.

3. Result and discussion

3.1. Characterization of AuE-L-Cys-GA-Gln Electrode

3.1.1. Cyclic voltammetry

The stepwise assembly of the layered functionalized electrode was traced by cyclic voltammetry (CV) and electrochemical impedance spectroscopy (EIS). CV is a useful technique that allows probing the features of modified electrode surfaces. The electrochemical responses at each step were investigated to confirm the layer-by-layer assembly process. Fig. 5(A) shows the voltammograms of the bare gold electrode (AuE) (curve a), the electrode modified with L-Cysteine (AuE-L-Cys) (curve b), activation with glutaraldehyde (AuE-L-Cys-GA) (curve c), and functionalization with glutamine (AuE-L-Cys-GA-Gln) (curve d) in the presence of the $[Fe(CN)_6^{3-/4-}$ redox probe. The reversible electrochemical behavior and large current density of the redox waves indicate that the redox couple can easily access the electrode surface of the bare Au electrode (Fig. 5 curve a). With the addition of the L-Cys monolayer onto the gold surface (curve b), activation with GA (curve c), and subsequent functionalization by Gln (curve d), it was observed that the peak current decreased and the irreversibility (ΔEp) of the redox probe reaction increased as a result of the layer-by-layer assembly (Fig. 5 curves b, c, and d). The results show that further layer-by-layer assembly on the electrode was influenced by the addition in chain length, which retards the interfacial electron transfer kinetics of the redox probe, resulting in the perturbation of the reversible behavior of the redox probe.

3.1.2. Impedance spectroscopy

Electrochemical methods are simple and low-cost methods for studying interfacial events at modified electrodes. Among these methods, EIS is a powerful, informative, and non-destructive technique that can be used to study interfacial events [66-71]. In this work, EIS measurements were used to trace events during the formation of the AuE/L-Cys/GA/Gln electrode and its interaction with the external probe. Fig. 5(B) shows the Nyquist plots of the bare AuE, AuE/L-Cys, AuE/L-Cys/GA, and AuE/L-Cys/GA/Gln electrodes.

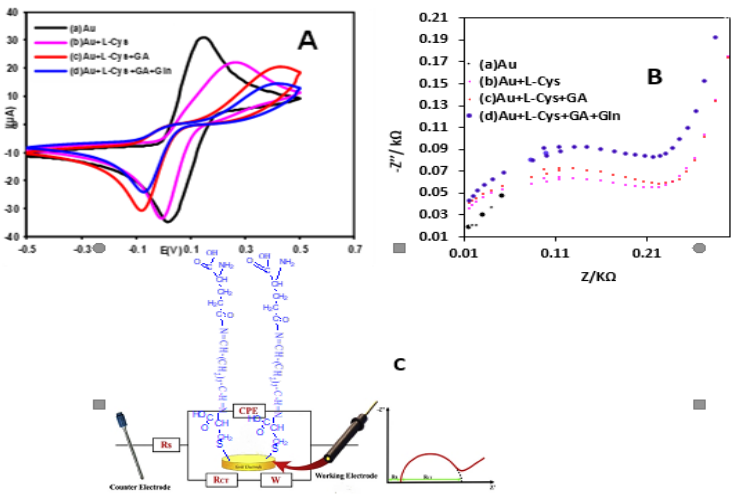

Fig. 5 CVs obtained for bare AuE (a), L-Cys/AuE (b) ,GA / L-Cys /AuE (c), Gln / GA / L-Cys /AuE(d) (B) Nyquist plots obtained for bare AuE(a) , L-Cys/AuE (b) GA / L-Cys /AuE(c) ,Gln/GA/L-Cys/AuE(d in the presence of the probe solution (C) Electrochemical impedance circuit model

An increase in charge transfer resistance is evident from the bare Au electrode to Au-Cys-GA-Gln due to the insulating effect of the SAM film. As seen, the semicircle appears from AuE to Au-Cys-GA-Gln electrodes, suggesting that the surface of the modified electrode exhibits more electron transfer resistance. The EIS data obtained on the modified Au-Cys-GA-Gln electrode in different steps are well approximated by the constant phase element (CPE) model (Fig. 5(C)).

3.2. Time

The modified electrode was immersed in a 5.0×10^{-4} M Cu^{2+} solution with pH 5.0 after adsorption of copper onto the electrode; DPV was obtained in the presence of CM. This work was repeated to absorb more copper at different times in the presence of CM. The maximum peak current was observed at 3 minutes.

3.3. PH

The effect of pH is one of the most important factors in measuring various compounds through electrochemical methods. Here, the effect of pH of the solution on the electrochemical behavior of CM (10 nM) in buffer (pH 5.5) was investigated by DP with a scan rate of 100 mV/s at the Au-Cys-GA-Gln-Cu^{2+}. The results are shown in Fig. 6. The highest current was observed at pH 5, which was used as the optimal pH for the measurement of CM by the electrocatalytic property of copper.

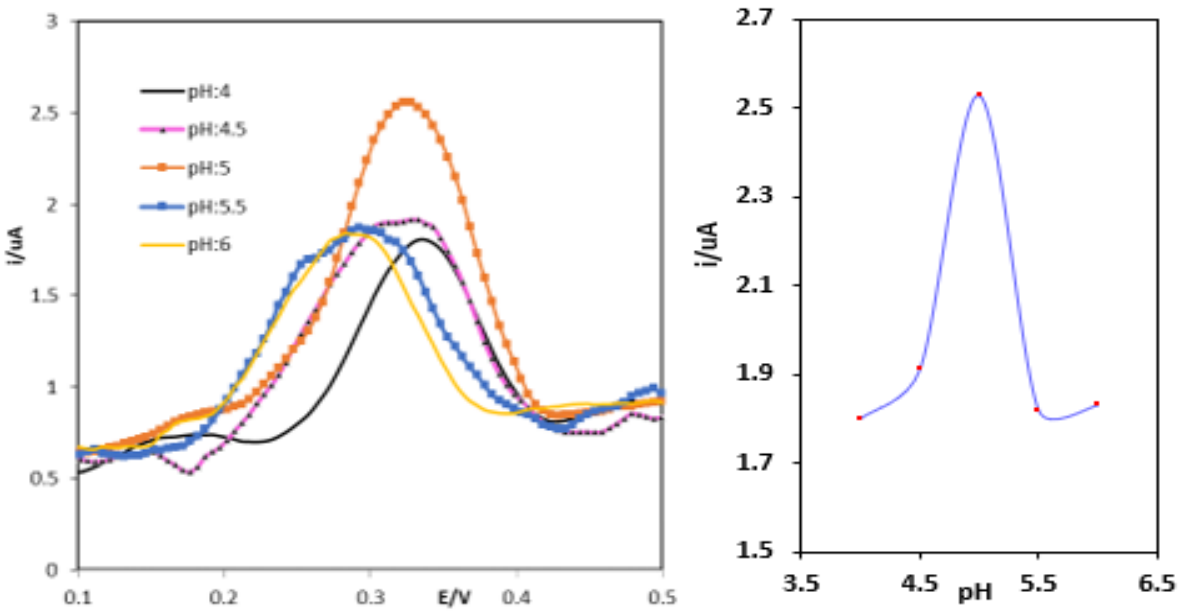

Fig. 6 Effect of pH on the oxidation of 0.1 μM CM

3.4. Calibration Curve, Detection Limit and Repeatability

Under optimized conditions, the DPVs by the modified electrode were obtained (Fig. 7). The DPV current around +292 mV in various concentrations of CM was recorded. Figure 4 (inset) shows that the DPV peak current is linear vs. pCM in the range of 1.0×10^{-6} - 1.0×10^{-10} M. The detection limit

calculated from the signal equals 3σ (standard deviation) of the background noise and was 1.3×10^{-11} M CM. The repeatability of the method was obtained for n = 9 at 1.0×10^{-7} M CM with a relative standard deviation (RSD) of 4.1%. The stability of the sensor was studied by comparing the electroanalytical response of the electrode for a series of repeated determinations.

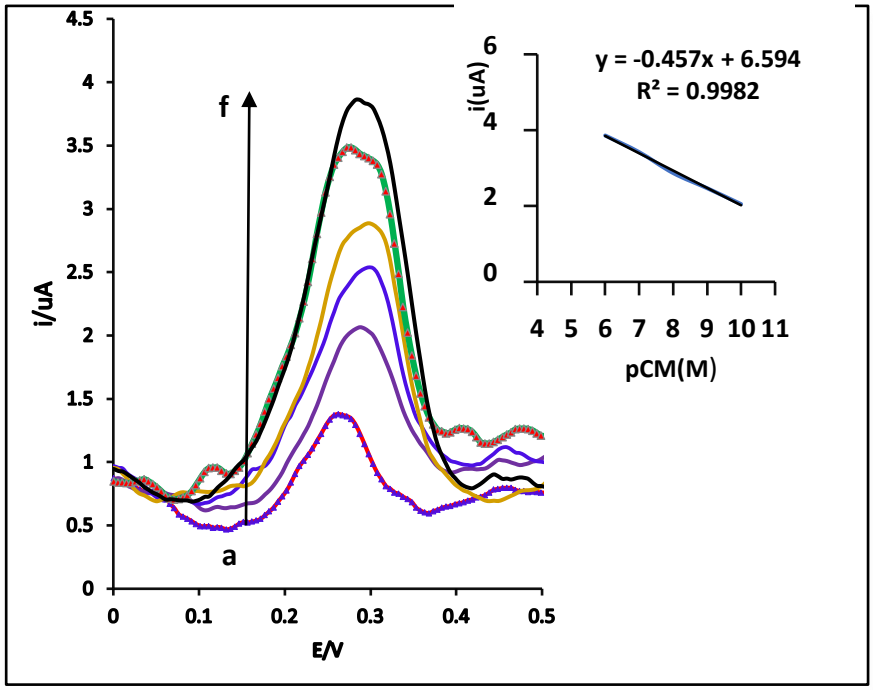

Fig. 7 (A) Differential pulse voltammograms obtained on Au-Cys-GA-Gln SAM modified electrode as a function of Cu^{2+} ion in the presence and absence of curcumin in concentrations: (a) 0.0, (b) 1.0×10^{-10}, (c) 1.0×10^{-9}, (d) 1.0×10^{-8}, (e) 1.0×10^{-7}, (f) 1.0×10^{-6} M in 0.1 M PBS (pH = 5), and 3 min accumulation time; (B) The inset shows calibration curve of Curcumin

3.5. Analysis of curcumin spiked in human blood serum

Curcumin levels in human blood serum were measured using Au-Cys-GA-Gln-Cu^{2+} in order to examine the effectiveness of the developed sensor in quantifying curcumin in actual samples. Blood serum was used to create experimental solutions with varying doses of curcumin. Following this, the DPVs of samples diluted with 0.1 M PBS (pH 5) were measured. The conventional addition technique was used to assess the curcumin recovery level. The findings shown in Table 1 show that the modified electrode maintained its efficiency for the accurate measurement of CM in a range of samples.

Table 1. Determination of Curcumin in real samples with the Cys-GA-Gln-Cu^{+2} modified gold electrode sensor.

Sample	Added (nM)	Found (nM)	Recovery (%)	RSD % (n = 3)
Human plasma	1.0	0.97	97.0	2.89
	5.0	5.2	104.0	2.73
	10.0	9.85	98.5	2.48

4. Conclutions

In this study, a novel electrochemical sensor utilizing a self-assembled monolayer of L-Cysteine-Glutaraldehyde-Glutamine-Cu^{2+} on a gold electrode was developed for the determination of curcumin in human blood serum. The modified electrode was successfully characterized using cyclic voltammetry (CV) and electrochemical impedance spectroscopy (EIS). The results demonstrated that the electrochemical activity of curcumin on the surface of the electrode modified with the L-Cysteine-Glutaraldehyde-Glutamine-Cu^{2+} self-assembled monolayer was

significantly better than that on the unmodified gold electrode (AuE). Compared to the bare AuE, the modified electrode exhibited a notable increase in the current of oxidation and reduction peaks.

The differential pulse voltammetry (DPV) method was employed to examine the electrochemical behavior of curcumin at the modified electrode. The highest oxidation current was obtained at pH 5 and a pre-concentration time of 180 seconds. The modified electrode was able to measure curcumin in real samples within the concentration range of 1×10^{-6} to 1×10^{-10} M, with a detection limit of 1.31×10^{-11} M The sensor displayed suitable stability, good sensitivity, and selectivity, making it an effective and inexpensive method for the determination of curcumin in human blood serum.

Conflict of interest: The authors declare that they have no conflict of interest.

References

1. Hewlings SJ, Kalman DS. Curcumin: A Review of Its Effects on Human Health. Foods. 2017;6:92.
2. Tabeshpour J, Hashemzaei M, Sahebkar A. Theregulatory role of curcumin on platelet functions. J Cell Biochem. 2018;119:8713–22.
3. Shrestha S, Zhu J, Wang Q, Du X, Liu F, Jiang J, et al. Melatonin potentiates the antitumor effect of curcumin by inhibiting IKKb/NF-kB/COX-2 signaling pathway. Int J Oncol. 2017;51:1249-60.
4. Ashrafizadeh M, Najafi M, Makvandi P, Zarrabi A, Farkhondeh T, Samarghandian S. Versatile role of curcumin and its derivatives in lung cancer therapy. J Cell Physiol. 2020;235:9241–68.
5. Hatcher H, Planalp R, Cho J. Curcumin: from ancient medicine to current clinical trials. Cellular Molec Life Sci. 2008;65:1631-52.
6. Roth GN, Chandra A, Nair MG. Novel bioactivities of Curcuma longa constituents. J Nat Prod. 1998;61:542-5.
7. Bhowmik CD. Kumar K, Chandira M. Turmeric: a herbal and traditional Medicine. Arch Appl Sci Res. 2009;1:86-108.
8. Anand P, Kunnumakkara A-B, Newman RA. Bioavailability of curcumin: problems and promises. Molec Pharmac. 2007;4:807-18.
9. Priyadarsini KI. The chemistry of curcumin: from extraction to therapeutic agent. Molecules. 2014;19:20091-112.
10. Kim YJ, Lee HJ, Shin Y. Optimization and validation of high-performance liquid. Agric Food Chem. 2013;61:10911-91.
11. Shishodia S, Sethi G, Aggarwal BB. Curcumin: getting back to the roots. Annals New York Acad Sci. 2005;1056:206-17.
12. Pulido-Moran M, Moreno-Fernandez F, Ramirez T. Curcumin and health. Molecules. 2016;21:264.
13. Singh S. From exotic spice to modern drug? Cell. 2007;130:765-8.
14. Gunes H, Gulen D, Mutlu R. Antibacterial effects of curcumin: an in vitro minimum inhibitory concentration study. Toxicology Ind Health. 2016;32:246-50.
15. Dhakal S, Chao K, Schmidt W. Evaluation of turmeric powder adulterated with metanil yellow using FT-Raman and FT-IR spectroscopy. Foods. 2016;5:36.
16. Krausz AE, Adler BL, Cabral V. Curcumin-encapsulated nanoparticles as innovative antimicrobial and wound healing agent, Nanomedicine: Nanotechnology. Biology Med. 2015;11:195-206.
17. Prasad S, Gupta SC, Tyagi AK. Curcumin, a component of golden spice: from bedside to bench and back. Biotech Adv. 2014;32:1053-64.
18. Beevers CS, Huang S. Pharmacological and clinical properties of curcumin, Botanics. Targets Therapy. 2011;1:5-18.
19. Aggarwal BB, Kumar A, Aggarwal MS. Curcumin derived from turmeric (Curcuma longa): a spice for all seasons. Phytopharmac Cancer Chemoprevention. 2005;23:351-87.
20. Nishiyama T, Mae T, Kishida,Curcuminoids H. Sesquiterpenoids inturmeric (Curcuma longa L.) suppress an increase in blood glucose level in type 2 diabetic KK-Ay mice. J Agric Food Chem. 2005;53:959-63.

21. Labban L. Medicinal and pharmacological properties of Turmeric (Curcuma longa): A review. Int J Pharm Biomed Sci. 2014;5:17-23.
22. Sreejayan N, Rao M, Priyadarsini K. Inhibition of radiation-induced lipid peroxidation by curcumin. Int J Pharmac. 1997;151:127-30.
23. Sharma R, Gescher A, Steward W. Curcumin: the story so far. Eur J Cancer. 2005;41:1955-68.
24. Delcea C, Siserman C. The emotional impact of COVID-19 on forensic staff. Rom J Leg Med. 2021 Mar 1;29(1):142-6.
25. Maheshwari RK, Singh AK, Gaddipati J. Multiple biological activities of curcumin: a short review. Life Sci. 2006;78:2081-7.
26. Aggarwal BB, Kumar A, Bharti AC. Anticancer potential of curcumin: preclinical and clinical studies. Anticancer Res. 2003;23:363-98.
27. Vică ML, Delcea C, Dumitrel GA, Vuşcan ME, Matei HV, Teodoru CA, Siserman CV. The influence of HLA alleles on the affective distress profile. Int J Environ Res Public Health. 2022 Oct 2;19(19):12608.
28. Yu H, Huang Q. Enhanced in vitro anti-cancer activity of curcumin encapsulated in hydrophobically modified starch. Food Chem. 2010;119:669-74.
29. Boon H, Wong J. Botanical medicine and cancer: a review of the safety and efficacy. Expert Opin Pharmacotherapy. 2004;5:2485-2501.
30. Sarkar FH, Li Y, Wang Z. Lesson learned from nature for the development of novel anti-cancer agents: implication of isoflavone,curcumin and their synthetic analogs. Curr Pharm Des. 2010;16:1801-1812.
31. Anand P, Sundaram C, Jhurani S. Curcumin and cancer: an “old-age”disease with an “age-old” solution. Cancer Lett. 2008;267:133-64.
32. Jurenka JS. Anti-inflammatory properties of curcumin, a major constituent of Curcuma longa: a review of preclinical and clinical research. Alternative Medicine Rev. 2009;142:141-53.
33. Lazaro M. Anticancer and carcinogenic properties of curcumin: considerations for its clinical development as a cancer chemopreventive and chemotherapeutic agent. Molec Nutrition Food Res. 2008;52:103-27.
34. Heath DD, Pruitt MA, Brenner E. Curcumin in plasma and urine:quantitation by high-performance liquid chromatography. J Chromatog B. 2003;783:287-95.
35. Lechtenberg M, Quandt B, Nahrstedt A. Quantitative determination of curcuminoids in Curcuma rhizomes and rapid differentiation of Curcuma domestica Val and Curcuma xanthorrhiza Roxb by capillary electrophoresis. Phytochem Anal. 2004;15:152-8.
36. Tang B, Ma L, Wang HY. Study on the supramolecular interaction of curcumin and β-cyclodextrin by spectrophotometry and its analytical application. J Agric Food Chem. 2002;50:1355-61.
37. Wang F, Huang W. Determination of curcumin by its quenching effect on the fluorescence of Eu^{3+}–tryptophan complex. J Pharmac Biomed Anal. 2007;43:393-8.
38. Peng J, Nong K, Cen L. Electropolymerization of acid chrome blue K on glassy carbon electrode for the determination of curcumin. J Chinese Chem Soc. 2012;59:1415-20.
39. Li K, Li Y, Yang L. The electrochemical characterization of curcumin and its selective detection in Curcuma using a graphene-modified electrode. Analyt Methods. 2014;6:7801-8.
40. Ezoji H, Rahimnejad M. Electrochemical Determination of Bisphenol A on Multi-Walled Carbon Nanotube/titanium dioxide Modified Carbon Paste Electrode. Int J Sci Res. 2016;7:242-6.
41. Heli H, Jabbari A, Majdi S. Electrooxidation and determination of some non-steroidal anti-inflammatory drugs on nanoparticles of Ni–curcumincomplex-modified electrode. J Solid State Electrochem. 2009;13:1951.
42. Daneshgar P, Norouzi P, Movahedi AM. Fabrication of carbonnanotube and dysprosium nanowire modified electrodes as a sensor for determination of curcumin. J Appl Electrochem. 2009;39:1983-1992.
43. Arslan E, Çakır S. A novel palladium nanoparticles-polyproline-modified graphite electrode and its application for determination of curcumin. J Solid State Electrochem. 2014;18:1611-20.
44. Rahimnejad M, Zokhtareh R, Moghadamnia AA, Asghary M. An Electrochemical Sensor Based on Reduced Graphene Oxide Modified Carbon Paste Electrode for Curcumin Determination in Human Blood Serum. Port Electrochim Acta. 2020;38:29-42.

45. Delcea C, Bululoi AS, Gyorgy M, Rad D. Psychological distress prediction based on maladaptive cognitive schemas and anxiety with random forest regression algorithm. Pharmacophore. 2023;14(5-2023):62-9.
46. Shervedani RK, Yaghoobi F, Mehrjardi AH, Barzoki SMS. Electrocatalytic activities of gold-5-amino-2-mercaptobenzimidazole-Mn+ self-assembled monolayer complexes (Mn+:Ag+, Cu2+) for hydroquinone oxidation investigated by CV and EIS, Electrochim. Acta 2008;53:4185-92.
47. Shervedani RK, Mozaffari SA. Copper(II) nanosensor based on a gold cysteamine self-assembled monolayer functionalized with salicylaldehyde. Anal Chem. 2006;78:4957–63.
48. Shervedani RK, Mehrjardi AHH, Zamiri N. A novel method for glucose determination based on electrochemical impedance spectroscopy using glucose oxidase self-assembled biosensor. Bioelectrochemistry. 2006;69:201–8.
49. Shervedani RK, Mehrjardi AHH. Comparative electrochemical behavior of glucose oxidase covalently immobilized on mono-, di- and tetra-carboxylic acid functional Au–thiol SAMs via anhydride–derivatization route. Sens Actuators B. 2009;137:195–204.
50. Shervedani RK, Bagherzadeh M. Hydroxamation of gold surface via in-situ layer by-layer functionalization of cysteamine self-assembled monolayer: preparation and electrochemical characterization. Electrochim Acta. 2008;53:6293–303.
51. Mandal S, Kazmi NH, Sayre LM. Ligand dependence in the copper-catalyzed oxidation of hydroquinones. Arch Biochem Biophys. 2005;435:21-31.
52. Owsik I, Kolarz B. The oxidation of hydroquinone to p-benzoquinone catalysed by Cu(II) ions immobilized on acrylic resins with aminoguanidyl groups: Part 1. J Mol Catal A Chem. 2002;178:63-71.
53. Shervedani RK, Mozaffari SA. Copper(II) nanosensor based on a gold cysteamine self-assembled monolayer functionalized with salicylaldehyde. Analytical Chemistry; 2006:78: 4957-4963.
54. Rosane I, de Oliveira WZ, de Barros Os´orio REM, Neves A, Vieira IC. Sensors Actuators B. 2007;122:89.
55. Shervedani RK, Yaghoobi F, Mehrjardi AH, Barzoki SM. A Hatefi-Mehrjardi, SM Siadat-Barzoki. Electrocatalytic activities of gold-5-amino-2-mercaptobenzimidazole-Mn^{+} self-assembled monolayer complexes (Mn^{+}: Ag^{+}, Cu^{2+}) for hydroquinone oxidation investigated by CV and EIS. Electrochimica Acta. 2008;53:4185-4192.
56. Wang S, Du D. Studies on the Electrochemical Behaviour of Hydroquinone at L-cysteine Self-Assembled Monolayers Modified Gold Electrode. Sensors. 2002;2:41-9.
57. Hashemi P, Afkhami A, Bagheri H, Amidi S, Madrakian T. Fabrication of a novel impedimetric sensor based on L-Cysteine/Cu(II) modified gold electrode for sensitive determination of ampyra. Analytica Chimica Acta. 2017;984:185-92.
58. Shervedani RK, Mozaffari SA. Copper(II) nanosensor based on a gold cysteamine selfassembled monolayer functionalized with salicylaldehyde. Anal Chem. 2006;78:4957-63.
59. Shervedani RK, Yaghoobi F, Mehrjardi AH, Barzoki SM. A Hatefi-Mehrjardi, SM Siadat-Barzoki. Electrocatalytic activities of gold-5-amino-2-mercaptobenzimidazole-Mn^{+} self-assembled monolayer complexes (Mn^{+}: Ag^{+}, Cu^{2+}) for hydroquinone oxidation investigated by CV and EIS. Electrochimica Acta. 2008;53:4185-4192.
60. Hoare JP. A cyclic voltammetric study of the gold oxygen system. J Electrochem Soc. 1984;131:1808-15.
61. Kumar A, Kaul S. Self-assembled monolayers on gold: Design and applications in electrochemistry. J Electroanal Chem. 2010;646:1-12.
62. Ulman A. Formation and structure of self-assembled monolayers. Chem Rev. 1996;96:1533-54.
63. Shervedani RK, Mozaffari SA. Copper(II) nanosensor based on a gold cysteamine self-assembled monolayer functionalized with salicylaldehyde. Anal Chem. 2006;78:4957-63.
64. Zhao C, Zhao J. Self-assembled monolayers of thiols on gold: A powerful platform for biosensing. Biosens Bioelectron. 2009;24:2366-75.
65. Brahma A, Vahdat M. Self-assembled monolayers as models for understanding interfacial phenomena. Langmuir. 2012;28:12251-61.

66. Macdonalds R, Janek RP, Fawcett WR. Evidence for complex double-layer structure in aqueous NaClO4 at the potential of zero charge. J Phys Chem. 1997;101:8550-58.
67. Zhou X, Yang Y, Yu Y. Electrochemical impedance spectroscopy: A versatile tool for the characterization of self-assembled monolayers on metal surfaces. Electrochim Acta. 2015;178:748-54.
68. Guan Y, Yang X, Ma H. Self-assembled monolayers on gold electrodes: Investigation by electrochemical impedance spectroscopy. J Phys Chem C. 2018;122:12340-48.
69. Bhanja P, Mukherjee S, Patra P. A comprehensive study on the formation and characterization of self-assembled monolayers using electrochemical impedance spectroscopy. Sens Actuators B Chem. 2019;298:126932.
70. Zhao Y, Liu J, Chen Y. Impedance spectroscopy for studying self-assembled monolayers: Insights into their electrochemical properties. Anal Chim Acta. 2021;1154:338-46.
71. Martínez-García G, Ruiz-García A, De La Fuente J. Electrochemical impedance spectroscopy as a tool for the characterization of self-assembled monolayers. Langmuir. 2023;39:1763-75.